# Mechanical, electronic, and optical properties of the A₄B₆ layered ferroelectrics: *ab initio* calculation

**Husnu Koc[1], Sevket Simsek[2], Selami Palaz[3], Oral Oltulu[3], Amirullah M. Mamedov*,[4,5], and Ekmel Ozbay[4]**

[1] Siirt University, Faculty of Science and Letters, Department of Physics, 56000 Siirt, Turkey
[2] Hakkari University, Faculty of Engineering, Department of Material Science and Engineering, 3000 Hakkari, Turkey
[3] Harran University, Faculty of Science and Letters, Department of Physics, 63000 Sanliurfa, Turkey
[4] Bilkent University, Nanotechnology Research Center, 06800 Ankara, Turkey
[5] Baku State University, International Scientific Center, Baku, Azerbaijan

* Corresponding author: e-mail mamedov@bilkent.edu.tr, Phone: +90 312 290 19 66, Fax: +90 312 266 40 42

We have performed a first principles study of the structural, elastic and electronic properties of orthorhombic SnS and GeS compounds using the density functional theory within the local density approximation. The second-order elastic constants have been calculated, and the other related quantities such as the Young's modulus, shear modulus, Poisson's ratio, anisotropy factor, sound velocities, Debye temperature, and hardness have also been estimated in the present work. All of the calculated modulus and Poisson's ratio for SnS were less than the same parameters for GeS. Our calculations have discovered the large anisotropy of elastic parameters in the (100) and (010)-planes for both compounds. The band structures of orthorhombic SnS and GeS have been calculated along high symmetry directions in the first Brillouin zone (BZ). The calculation results for the band gap of Sn(Ge)S gave $E_g$=0.256 eV (0.852 eV) and has an indirect character for an interband transition. The real and imaginary parts of dielectric functions and (by using these results) the optical constant such as energy-loss function, the effective number of valance electrons and the effective optical dielectric constant were calculated. All of the principal features and singularities of the dielectric functions for both compounds were found in the energy region between 2 eV and 20 eV.

**1 Introduction** SnS and GeS, the members of compounds with the general formula A⁴B⁶ (A=Ge, Sn, Pb and B=S, Se, Te), are the metal chalcogenide structures with an orthorhombic layered crystal structure. SnS and GeS structures consist of double layers of atoms, with each Ge (Sn) atom coordinated by two S atoms in the plane of the layer [1]. These compounds possess an orthorhombic crystal structure with eight atoms per unit cell belonging to the space group Pnma. These layered semiconductors have been attracting the attention of scientists because of their potential application in optoelectronic devices [2].

In the past, some detailed works [1-7] have been carried out on the structural and electronic properties of these compounds. Rathor et al. [3] presented the bands and density of states (DOS) using the Hartree-Fock, density functional and pseudopotential schemes. Gashimzade et al. [4]

calculated the phonon modes of IV-VI semiconductor crystals (GeS, GeSe, SnS, and SnS) using the density functional perturbation theory (DEPT). Waghmare et al. [5] calculated the phonon frequencies, electron localization lengths, Born effective charges, dielectric response, and conventional electronic structures of the IV-VI chalcogenide series using the first principle density functional theory. Wiedemeier et al. [6] refined the structures of GeS, GeSe, SnS, and SnSe using the X-ray diffractometer. Malone et al. [7] performed the electronic structures of SnS and GeS materials using the density functional theory calculation. Band gap corrections of these materials are computed within the GW approximation. Rajagopalan et al. [2] investigated the structural behaviour of SnS under pressure using the first principle density functional calculations. Ettoma et al. [1] presented the electronic band structure of

SnS using the ab initio band structure calculation and photoelectron spectroscopy methods.

As far as we know, no ab initio general potential calculations of the mechanical properties and detail optical properties such as the energy-loss function, the effective number of valance electrons and the effective optical dielectric constant along the main crystallographic axes of the SnS and GeS have been reported. The main purpose of this work is to provide some additional information on the existing features of SnS and GeS by using the density functional theory. Therefore, in this work, we have investigated the structural, electronic, mechanical, and photon energy-dependent optical properties of the SnS and GeS crystals. The method of calculation is given in Section 2; the results are discussed in Section 3. Finally, the summary and conclusion are given in Section 4.

## 2 Model and method

Our calculations have been performed using the density functional formalism and local density approximation (LDA) [8] through the Ceperley and Alder functional [9] as parameterized by Perdew and Zunger [10] for the exchange-correlation energy in the SIESTA code [11, 12]. This code calculates the total energies and atomic forces using a linear combination of atomic orbitals as the basis set. The basis set is based on the finite range pseudoatomic orbitals (PAOs) of the Sankey-Niklewsky type [13], generalized to include multiple-zeta decays.

The interactions between electrons and core ions are simulated with separable Troullier-Martins norm-conserving pseudopotentials [14]. We have generated atomic pseudopotentials separately for atoms, Sn, Ge and S by using the $5s^25p^2$, $4s^24p^2$ and $3s^23p^4$ configurations, respectively. For present atomic pseudopotentials, the cut-off radii are taken as s: 2.40 au, p: 2.46 au, 2.79 au for the d and f channels of Sn, s: 2.06 au, p: 2.85 au, 2.58 au for the d and f channels of Ge and s: 1.60 au, p: 1.73 au, 1.90 au for the d and f channels of S. Siesta calculates the self-consistent potential on a grid in real space. The fineness of this grid is determined in terms of an energy cut-off $E_c$ in analogy to the energy cut-off when the basis set involves plane waves. Here, by using a double-zeta plus polarization (DZP) orbitals basis and the cut-off energies between 100 and 500 R with various basis sets, we found an optimal value of around 350 R for SnS and GeS. 75 k-points for SnS and GeS were enough to obtain the converged total energies.

## 3 Results and discussion

**3.1 Structural properties** The structures of SnS and GeS are considered as an orthorhombic structure. These crystals have four molecules (8 atoms) in the unit cell. The equilibrium lattice parameters were obtained by minimizing the total energy for the different values of the lattice parameters by means of Murnaghan's equation of states (EOS) [15]. The results are shown in Table 1. The obtained

lattice parameters are in good agreement with the experimental and theoretical values.

**Table 1** The calculated equilibrium lattice parameters (a, b, and c), with the theoretical and experimental values for SnS and GeS in fractional coordinates.

| Material | Reference | $a$ (Å) | $b$ (Å) | $c$ (Å) |
|---|---|---|---|---|
| SnS | Present | 4.309 | 11.136 | 3.964 |
| | Exp. [6] | 4.388 | 11.200 | 3.987 |
| | Exp. [15] | 4.34 | 11.20 | 3.99 |
| | Theory [7] | 4.334 | 10.91 | 3.88 |
| | | | | |
| | Present | 4.268 | 10.406 | 3.619 |
| | Exp. [6] | 4.299 | 10.481 | 3.646 |
| | Exp. [15] | 4.30 | 10.47 | 3.64 |
| | Theory [7] | 4.29 | 10.22 | 3.51 |

**3.2 Elastic properties** The elastic constant $C_{ij}$ of solids provides a link between the mechanical and dynamical behavior of crystals, and some of the most important information that can be obtained from ground state total energy calculations. The $C_{ij}$ determine the response of the crystal to external forces characterized by the bulk modulus, Young's modulus, shear modulus, and Poisson's ratio, and, therefore, play an important part in determining the stability and stiffness of the materials [16-18]. The present elastic constants are computed by using the "volume-conserving" technique [19]. The obtained $C_{ij}$ calculations are summarized in Table 2. Unfortunately, there are no theoretical results for comparing them with the present work. However, our results can serve as a prediction for future investigations.

Nine independent strains are necessary to compute the elastic constants of orthorhombic GeS and SnS compounds. Mechanical stability leads to restrictions on the elastic constants, which for orthorhombic crystals [19-21] are

$$(C_{11} + C_{22} - 2C_{12}) > 0 , \ (C_{11} + C_{33} - 2C_{13}) > 0 ,$$

$$(C_{22} + C_{33} - 2C_{23}) > 0 , \ C_{11} > 0, C_{22} > 0, \quad (1)$$

$$C_{33} > 0, \ C_{44} > 0, \ C_{55} > 0, \ C_{66} > 0,$$

$$(C_{11} + C_{22} + C_{33} + 2C_{12} + 2C_{13} + 2C_{23}) > 0 .$$

The present elastic constants in Table 2 obey these stability conditions for orthorhombic SnS and GeS. The elastic constants $C_{11}$, $C_{22}$, and $C_{33}$ measure the $a$-, $b$-, and $c$-direction resistance to linear compression, respectively. The $C_{11}$ for SnS and GeS compounds are lower than the $C_{22}$ and $C_{33}$. Thus, SnS and GeS compounds are more compressible along the a-axis. It is known that the elastic constant $C_{44}$ is the most important parameter indirectly governing the indentation hardness of a material. The large $C_{44}$ means a strong ability of resisting the monoclinic shear distortion in (100) plane, and $C_{66}$ relates to the resistance to shear in the <110> direction. In the present case, $C_{44}$ and $C_{66}$ for GeS are higher than the SnS compound.

Phys. Status Solidi C **12**, No. 6 (2015)

653

**Table 2** The calculated elastic constants (in GPa) for SnS and GeS

| Material | Reference | $C_{11}$ | $C_{22}$ | $C_{33}$ | $C_{12}$ | $C_{13}$ | $C_{23}$ | $C_{44}$ | $C_{55}$ | $C_{66}$ |
|---|---|---|---|---|---|---|---|---|---|---|
| SnS | Present | 99.34 | 137.58 | 106.62 | 26.23 | 52.17 | 21.86 | 36.27 | 77.48 | 38.53 |
| GeS | Present | 122.9 | 169.08 | 145.80 | 34.78 | 54.0 | 34.04 | 48.81 | 93.0 | 50.79 |

**Table 3** The calculated isotropic bulk modulus (B, in GPa), shear modulus (G, in GPa), Young's modulus (E, in GPa) and Poisson's ratio  for SnS and GeS compounds.

| Material | Reference | $B_R$ | $B_V$ | $B$ | $G_R$ | $G_V$ | $G$ | $E$ | $\upsilon$ |
|---|---|---|---|---|---|---|---|---|---|
| SnS | Present | 60.41 | 60.45 | 60.43 | 40.33 | 46.67 | 43.50 | 105.3 | 0.2097 |
| GeS | Present | 75.65 | 75.93 | 75.79 | 54.58 | 59.52 | 57.05 | 136.8 | 0.1991 |

A problem arises when single crystal samples are not available, since it is then not possible to measure the individual elastic constants. Instead, the polycrystalline bulk modulus ( $B$ ) and shear modulus ( $G$ ) may be determined. There are two approximation methods to calculate the polycrystalline modulus, namely, the Voigt method [22] and the Reuss method [23]. For specific cases of orthorhombic lattices, the Reuss shear modulus ( $G_R$ ) and the Voigt shear modulus ( $G_V$ ) are

$$G_R = 15 \left\{ \begin{array}{l} [C_{11}(C_{22}+C_{33}+C_{23})+C_{22}(C_{33}+C_{13}) \\ +C_{33}C_{12}-C_{12}(C_{23}+C_{12})-C_{13}(C_{12}+C_{13}) \\ -C_{23}(C_{13}+C_{23})]/\Delta + 3[(1/C_{44}) \\ +(1/C_{55})+(1/C_{66})] \end{array} \right\}^{-1} \quad (2)$$

and

$$G_V = \frac{1}{15}(C_{11}+C_{22}+C_{33}-C_{12}-C_{13}-C_{23}) \\ + \frac{1}{5}(C_{44}+C_{55}+C_{66}) \quad (3)$$

and the Reuss bulk modulus ( $B_R$ ) and Voigt bulk modulus ( $B_V$ ) are defined as

$$B_R = \Delta \left[ \begin{array}{l} C_{11}(C_{22}+C_{33}-2C_{23})+C_{22}(C_{33}-2C_{13}) \\ -2C_{33}C_{12}+C_{12}(2C_{23}-C_{12}) \\ +C_{13}(2C_{12}-C_{13})+C_{23}(2C_{13}-C_{23}) \end{array} \right]^{-1} \quad (4)$$

and

$$B_V = \frac{1}{9}(C_{11}+C_{22}+C_{33}) + \frac{2}{9}(C_{12}+C_{13}+C_{23}). \quad (5)$$

In Eq. (2) and (4),
$\Delta = C_{13}(C_{12}C_{23}-C_{13}C_{22})+C_{23}(C_{12}C_{13}-C_{23}C_{11})+C_{33}(C_{11}C_{22}-C_{12}^2)$ is the elastic compliance constant. Using energy considerations Hill [24] proved that the Voigt and Reuss equations represent the upper and lower limits of the true polycrystal-

line constants, and recommended that a practical estimate of the bulk and shear moduli were the arithmetic means of the extremes. Hence, the elastic moduli of the polycrystalline material can be approximated by Hill's average. The shear moduli can, therefore, be expressed as

$$G = \frac{1}{2}(G_R + G_V), \quad (6)$$

and in a similar manner  the  bulk moduli  can be written as

$$B = \frac{1}{2}(B_R + B_V). \quad (7)$$

Young's modulus, $E$, and Poisson's ratio, $v$, for an isotropic material are given by

$$E = \frac{9BG}{3B+G}, \quad (8)$$

$$v = \frac{3B-2G}{2(3B+G)}, \quad (9)$$

respectively [25, 26]. The Hill average [24] was used to calculate the polycrystalline modulus in a manner similar to our recent works [17, 18].Using the relations given above, the calculated bulk modulus, shear modulus, Young's modulus, and Poisson's ratio for SnS and GeS are given in Table 3. The bulk modulus is a measure of resistance to volume change by an applied pressure, whereas the shear modulus is a measure of resistance to reversible deformations upon shear stress [27]. Hence, shear modulus exhibits better correlations with hardness than the bulk modulus. The calculated bulk modulus and shear modulus for SnS and GeS are 60.43, 43.50 GPa and 75.79, 57.05 GPa, respectively. The values of the bulk moduli indicate that GeS is a less compressible material than the SnS compound. The calculated shear modulus for SnS is lower than GeS compound.

The criterion in Refs. [27, 28] for ductility or brittleness is the value of the $B/G$. If the $B/G$ ratio is higher (less) than, 1.75, then a material is ductile (brittle). The $B/G$ ratio calculated for SnS and GeS compounds are lower than 1.75. Hence, both compounds behave in a brittle manner.

Young's modulus, which is defined as the ratio of stress to strain for a given material, is used to provide for the measurement of the stiffness of the solid. The higher the value of Young's modulus, the stiffer the materials will be. Here, the value of Young's modulus (105.3 GPa) of the SnS compound is higher than GeS (136.8 GPa). Therefore, the GeS compound is relatively stiffer than SnS. If the value of $E$, which has an impact on the ductile, increases, then the covalent nature of the material also increases. In Table 3, it is shown that $E$ increases as you move from SnS to GeS. The value of Poisson's ratio is indicative of the degree of directionality of the covalent bonds. The value of the Poisson's ratio is small ($\upsilon$ =0.1) for covalent materials, whereas for ionic materials a typical value of $\upsilon$ is 0.25 [29]. The calculated Poisson's ratios are approx. 0.210 and 0.199 for SnS and GeS, respectively. Therefore, the ionic contribution to inter atomic bonding for these compounds is dominant. The $\upsilon$=0.25 and 0.5 are the lower and upper limits, respectively, for central force solids [30]. For SnS and GeS, the values of $\upsilon$ are close to 0.25, indicating that interatomic forces are central forces.

In the crystal structures, elastic anisotropy is important in understanding the elastic properties [31]. The shear anisotropic factors on different crystallographic planes provide a measure of the degree of anisotropy in atomic bonding in different planes. The shear anisotropic factors are given by

$$A_1 = \frac{4C_{44}}{C_{11} + C_{33} - 2C_{13}} \quad \text{for the \{100\} plane,} \quad (10)$$

$$A_2 = \frac{4C_{55}}{C_{22} + C_{33} - 2C_{23}} \quad \text{for the \{010\} plane,} \quad (11)$$

$$A_3 = \frac{4C_{66}}{C_{11} + C_{22} - 2C_{12}} \quad \text{for the \{001\} plane.} \quad (12)$$

The calculated values of $A_1, A_2$ and $A_3$ for SnS and GeS are given in Table 4. A value of unity means that the crystal exhibits isotropic properties while values other than unity represent varying degrees of anisotropy. From Table 4, it can be seen that SnS and GeS exhibit larger anisotropy in the {100} and {010} planes and these compounds exhibit almost isotropic properties for the {001} plane according to other planes. Another way of measuring the elastic anisotropy is given by the percentage of anisotropy in the compression and shear [29, 30, 32].

$$A_{comp} = \frac{B_V - B_R}{B_V + B_R} \times 100, \quad (13)$$

$$A_{shear} = \frac{G_V - G_R}{G_V + G_R} \times 100. \quad (14)$$

For crystals, these values can range from zero (isotropic) to 100% representing the maximum anisotropy. The percentage anisotropy values have been computed for SnS and GeS, and are shown in Table 4. It can be also seen that

the anisotropy of SnS in compression is small and its anisotropy in shear exhibits relatively high shear compared to GeS.

**Table 4** The shear anisotropic factors A$_1$, A$_2$, A$_3$, and A$_{comp}$(%), A$_{shear}$(%).

| Material | Reference | $A_1$ | $A_2$ | $A_3$ | $A_{comp}$ | $A_{shear}$ |
|----------|-----------|-------|-------|-------|------------|-------------|
| SnS | Present | 1.43 | 1.55 | 0.84 | 0.03 | 7.29 |
| GeS | Present | 1.06 | 1.51 | 0.91 | 0.18 | 4.33 |

**Table 5** The longitudinal, transverse, average elastic wave velocities, and hardness together with the Debye temperature for SnS and GeS.

| Material | Reference | $v_l$ (m/s) | $v_t$ (m/s) | $v_m$ (m/s) | $\theta_D$ (K) |
|----------|-----------|-------------|-------------|-------------|----------------|
| SnS | Present | 4745 | 2875 | 3178 | 414 |
| GeS | Present | 5928 | 3634 | 4011 | 553 |

One of the standard methods for calculating the Debye temperature is to use elastic constant data since $\theta_D$ [33] may be estimated from the average sound velocity ($v_m$).

$$\theta_D = \frac{\hbar}{k} \left[ \frac{3n}{4\pi} \left( \frac{N_A \rho}{M} \right) \right]^{1/3} v_m, \quad (15)$$

where $\hbar$ is Planck's constants, $k$ is Boltzmann's constant, $N_A$ is Avogadro's number, $n$ is the number of atoms per formula unit, $M$ is the molecular mass per formula unit, $\rho (= M/V)$ is the density, and $v_m$ is given [34] as

$$v_m = \left[ \frac{1}{3} \left( \frac{2}{v_t^3} + \frac{1}{v_l^3} \right) \right]^{-1/3}, \quad (16)$$

where $v_l$ and $v_t$, are the longitudinal and transverse elastic wave velocities, respectively, which are obtained from Navier's equation [35]

$$v_l = \sqrt{\frac{3B + 4G}{3\rho}}, \quad (17)$$

and

$$v_t = \sqrt{\frac{G}{\rho}}. \quad (18)$$

At low temperatures, we have calculated the sound velocities and the Debye temperature by using the common relation given herein above for SnS and GeS, and the results are listed in Table 5. For materials, usually, the higher Debye temperature, the larger microhardness. The calculated Debye temperature for GeS is higher than SnS. Unfortunately, there are no theoretical and experimental results to compare with the calculated $v_l$, $v_t$, $v_m$, and $\theta_D$ values.

Phys. Status Solidi C **12**, No. 6 (2015)

655

**Table 6** Energy band gap for SnS and GeS Debye temperature for GeS is higher than SnS. Unfortunately, there are no theoretical and experimental results to compare with the calculated $v_l$, $v_t$, $v_m$, and $\theta_D$ values.

| Material | Reference | $E_g(eV)$ |
|---|---|---|
| SnS | Present | 0.256 indirect |
| | Theory (DFT-LDA) [7] | 0.4 indirect |
| | Experimental [6] | 0.72 |
| | | |
| GeS | Present | 0.852 indirect |
| | Theory (DFT-LDA) [3] | 0.73 direct, 0.83 indirect |
| | Theory (DFT-GGA) [3] | 0.83 direct, 0.89 indirect |
| | Theory (FP-LAPW with GGA) [3] | 1.051 direct, 1.053 indirect |
| | Theory (FP-LAPW with GGA) [36] | 1.10 indirect, 1.12 direct |
| | Theory (FP-LAPW with GGA) [15] | 1.52 indirect |
| | Experimental [37] | 1.65 direct |
| | Experimental [38] | 1.65 direct |
| | Experimental [39] | 1.54 indirect |

**3.3 Electronic properties** The investigation of the electronic band structure for understanding the electronic and optical properties of SnS and GeS is very useful. The band structures of the orthorhombic SnS and GeS were calculated using LDA approximation. The electronic band structures were calculated along the special lines connecting the high-symmetry points Γ (0,0,0), X (½,0,0), S (½,½,0), Y (0,½,0), Z (0,0, ½), R (½,½,½) for SnS and GeS in the k-space.
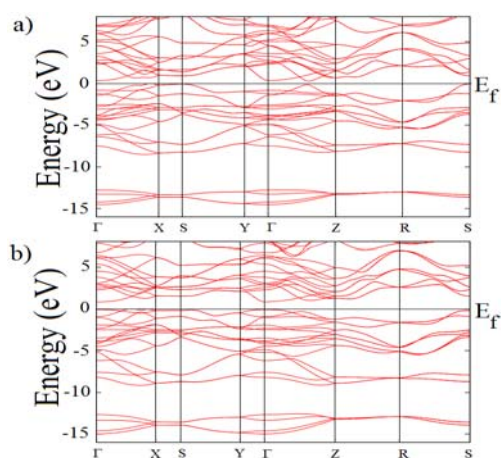


**Figure 1** Energy band structure for a) SnS and b) GeS

The energy band structures calculated for SnS and GeS are shown in Fig. 1. As can be seen in Fig. 1a, the SnS compound is an indirect band gap semiconductor with the value 0.256 $eV$ (see Table 6). The top of the valance band positioned at the nearly X point between Γ and X point of BZ, the bottom of the conduction band is located at the nearly Z point between Γ and Z point of BZ. The band gap with the value 0.852 $eV$ (see Table 6) of GeS compound has the same character of that of SnS. Similarly, the top of the valance band is located at the nearly midway point between Γ and X point of the BZ, and the bottom of the conduction band is located at the Γ point of BZ. The

band gap value obtained for GeS is in good agreement with the theoretical results, but is less than the estimated experimental results. The present band and the density of states (DOS) profiles for GeS agree with the earlier work [1, 7]. The total and partial densities of states corresponding to the band structures of SnS and GeS were calculated and the results are indicated in Fig. 2 and Fig. 3 along with the Fermi energy level, respectively. In these figures, the lowest valence bands that occur between approximately -16 and -12 $eV$ are dominated by S 3s states while the valence bands that occur between approximately -10 and -6 $eV$ are dominated by Sn 5s and Ge 4s states. The highest occupied valance bands are essentially dominated by S 3p states. The 5p and 4p states of Sn and Ge atoms, respectively are also contributing to the valance bands, but the values of the densities of these states are rather small compared to S 3p states. The lowest unoccupied conduction bands just above Fermi energy level is also dominated by the 5p and 4p states of Sn and Ge atoms, respectively.

**3.4 Optical properties** It is well known that the effect of the electric field vector, $E(\omega)$, of the incoming light is to polarize the material. At the level of linear response, this polarization can be calculated using the following relation [40, 41]:

$$P^i(\omega) = \chi_{ij}^{(1)}(-\omega,\omega)E^j(\omega), \qquad (19)$$

where $\chi_{ij}^{(1)}$ is the linear optical susceptibility tensor and it is given by [42]

$$\chi_{ij}^{(1)}(-\omega,\omega) = \frac{e^2}{\hbar\Omega}\sum_{nm\vec{k}} f_{nm}(\vec{k})\frac{r_{nm}^i(\vec{k})r_{mn}^i(\vec{k})}{\omega_{mn}(\vec{k})-\omega} = \frac{\varepsilon_{ij}(\omega)-\delta_{ij}}{4\pi} \quad (20)$$

where $n, m$ denote energy bands, $f_{mn}(\vec{k}) \equiv f_m(\vec{k}) - f_n(\vec{k})$ is the Fermi occupation factor, $\Omega$ is the normalization volume, $\omega_{mn}(\vec{k}) \equiv \omega_m(\vec{k}) - \omega(\vec{k})$ are the frequency differences, $\hbar\omega_n(\vec{k})$ is the energy of band $n$ at wave vector **k**. The $\vec{r}_{nm}$ are the matrix elements of the position operator
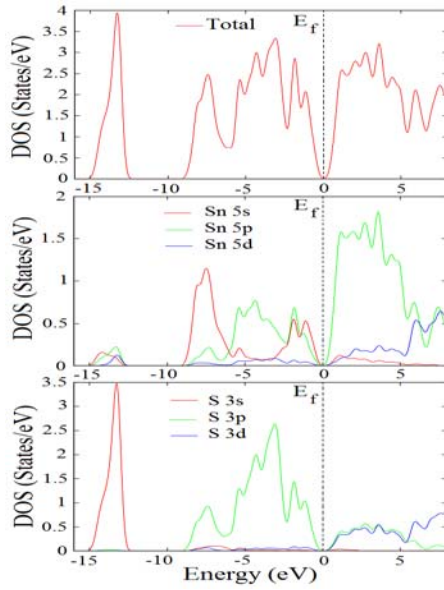
**Figure 2** The total and projected density of states for SnS.
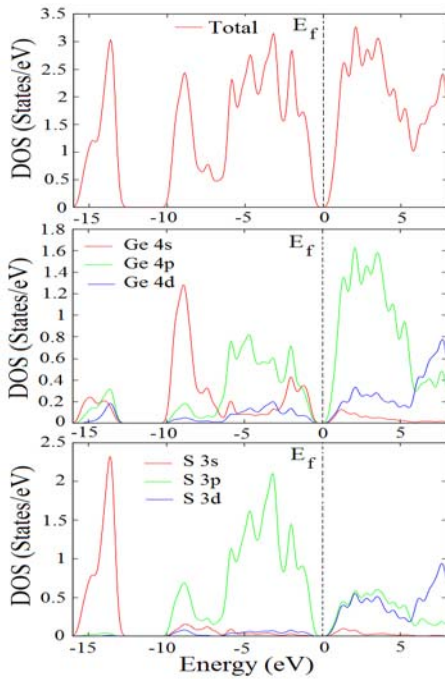


**Figure 3** The total and projected density of states for GeS.

[42]. As can be seen from Eq. (20), the dielectric function $\varepsilon_{ij}(\omega) = 1 + 4\pi\chi_{ij}^{(1)}(-\omega, \omega)$ and the imaginary part of $\varepsilon_{ij}(\omega)$, $\varepsilon_2^{ij}(\omega)$, is given by

$$\varepsilon_2^{ij}(w) = \frac{e^2}{\hbar\pi} \sum_{nm} \int d\vec{k} f_{nm}(\vec{k}) \frac{v_{nm}^i(\vec{k}) v_{nm}^j(\vec{k})}{\omega_{mn}^2} \delta(\omega - \omega_{mn}(\vec{k})). \quad (21)$$

The real part of $\varepsilon_{ij}(\omega)$ and $\varepsilon_1^{ij}(\omega)$ can be obtained by using the Kramers-Kroning transformation [42]. Because the

Kohn-Sham equations determine the ground state properties, the unoccupied conduction bands as calculated have no physical significance. If they are used as single-particle states in a calculation of the optical properties for semiconductors, a band gap problem comes included in the calculations of response.

The known sum rules [43] can be used to determine some quantitative parameters, particularly the effective number of the valence electrons per unit cell $N_{eff}$, as well as the effective optical dielectric constant $\varepsilon_{eff}$, which make a contribution to the optical constants of a crystal at the energy $E_0$. One can obtain an estimate of the distribution of oscillator strengths for both intraband and interband transitions by computing the $N_{eff}(E_0)$ defined according to

$$N_{eff}(E) = \frac{2m\varepsilon_0}{\pi\hbar^2 e^2 Na} \int_0^\infty \varepsilon_2(E) E dE, \quad (22)$$

where $N_a$ is the density of atoms in a crystal, $e$ and $m$ are the charge and mass of the electron, respectively and $N_{eff}(E_0)$ is the effective number of electrons contributing to optical transitions below an energy of $E_0$.

Further information on the role of the core and semicore bands may be obtained by computing the contribution that the various bands make to the static dielectric constant, $\varepsilon_0$. According to the Kramers-Kronig relations, $\varepsilon_0$ can be written in the form

$$\varepsilon_0(E) - 1 = \frac{2}{\pi} \int_0^\infty \varepsilon_2(E) E^{-1} dE. \quad (23)$$

One can, therefore, define an 'effective' dielectric constant, which represents a different mean of the interband transitions from that represented by the sum rule, Eq. (23), according to the relation

$$\varepsilon_{eff}(E) - 1 = \frac{2}{\pi} \int_0^{E_0} \varepsilon_2(E) E^{-1} dE. \quad (24)$$

The physical meaning of $\varepsilon_{eff}$ is quite clear: $\varepsilon_{eff}$ is the effective optical dielectric constant governed by the interband transitions in the energy range from zero to $E_0$, i.e. by the polarizition of the electron shells. In order to calculate the optical response by using the calculated band structure, we have chosen a photon-energy range of 0-25 $eV$ and have seen that a 0-15 $eV$ photon-energy range is sufficient for most optical functions.

The SnS and GeS single crystals have an orthorhombic structure that is optically a biaxial system. For this reason, the linear dielectric tensor of the SnS and GeS compounds have three independent components that are the diagonal elements of the linear dielectric tensor. We first calculated the real and imaginary parts of the linear dielectric function of the SnS and GeS compounds along the x- and z-directions (Fig. 4 and Fig. 5). All of the SnS and GeS
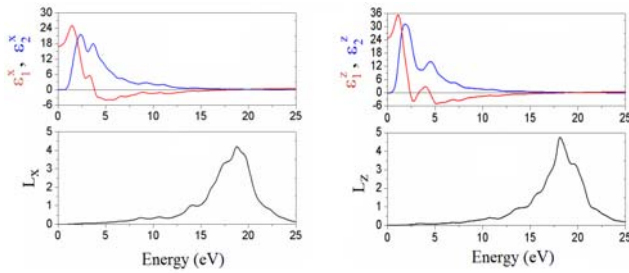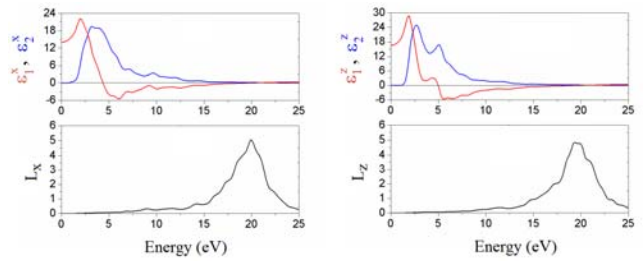
**Figure 4** Energy spectra of dielectric function $\varepsilon = \varepsilon_1 - i\varepsilon_2$ and energy-loss function (L) along the x- and z-axes for SnS.

compounds studied so far have $\varepsilon_1^x\left(\varepsilon_1^z\right)$ and are equal to zero in the energy region between 2 $eV$ and 19 $eV$ for decreasing ($d\varepsilon_1/dE < 0$) and increasing ($d\varepsilon_1/dE > 0$) of $\varepsilon_1(eV)$ (see Table 7). In addition, the values of $\varepsilon_1$ versus photon energy have main peaks in the energy region between 0.5 $eV$ and 6 $eV$. Some of the principal features and singularities of the $\varepsilon_{ij}$ for both investigated co pounds are shown in Table 7. The peaks of the $\varepsilon_2^x$ and $\varepsilon_2^z$ correspond to the optical transitions from the valence band to the conduction band and are in an agreement with the previous result [36, 37] for GeS. The maximum peak values of $\varepsilon_2^x$ and $\varepsilon_2^z$ for SnS are around 2.37 $eV$ and 1.88 $eV$, respectively, whereas the maximum values of $\varepsilon_2^x$ and $\varepsilon_2^z$ for GeS are around 3.18 $eV$ and 2.69 $eV$, respectively. In general, there are various contributions to the dielectric function, but Fig. 4 and Fig. 5 show only the contribution of the electronic polarizability to the dielectric function. In the range between 1 $eV$ and 5 $eV$, $\varepsilon_1^z$ decrease with increasing photon-energy, which is characteristic of an anomalous dispersion. In this energy range, the transitions between occupied and unoccupied states mainly occur between occupied and unoccupied S 3p states that can be seen in the DOS and PDOS shown in Fig. 2 and Fig. 3.

**Table 7** Some of principal features and singularities of the linear optical responses for SnS and GeS.

| Material | $\varepsilon_1(eV)$ | $d\varepsilon_1/dE < 0$ | | $d\varepsilon_1/dE > 0$ | | $\varepsilon_2(eV)$ | |
|---|---|---|---|---|---|---|---|
| SnS | $\varepsilon_1^x$ | 3.84 | - | 17.88 | - | $\varepsilon_{2,max}^x$ | 2.37 |
| | $\varepsilon_1^z$ | 2.41 | 4.49 | 3.27 | 18.04 | $\varepsilon_{2,max}^z$ | 1.88 |
| GeS | $\varepsilon_1^x$ | 4.41 | - | 19.47 | - | $\varepsilon_{2,max}^x$ | 3.18 |
| | $\varepsilon_1^z$ | 5.02 | - | 19.27 | - | $\varepsilon_{2,max}^z$ | 2.69 |



**Figure 5** Energy spectra of dielectric function $\varepsilon = \varepsilon_1 - i\varepsilon_2$ and energy-loss function (L) along the x- and z-axes for GeS.

The corresponding energy-loss functions, $L(\omega)$, are also presented in Fig. 4 and Fig. 5. In this figure, $L_x$ and $L_z$ correspond to the energy-loss functions along the x- and z-directions. The function $L(\omega)$ describes the energy loss of fast electrons traversing the material. The sharp maxima in the energy-loss function are associated with the existence of plasma oscillations [44]. The curves of $L_x$ and $L_z$ in Fig. 4 and Fig. 5 have a maximum near 18.77 and 18.16 $eV$ for SnS, respectively, and 19.96 and 19.35 $eV$ for GeS, respectively.
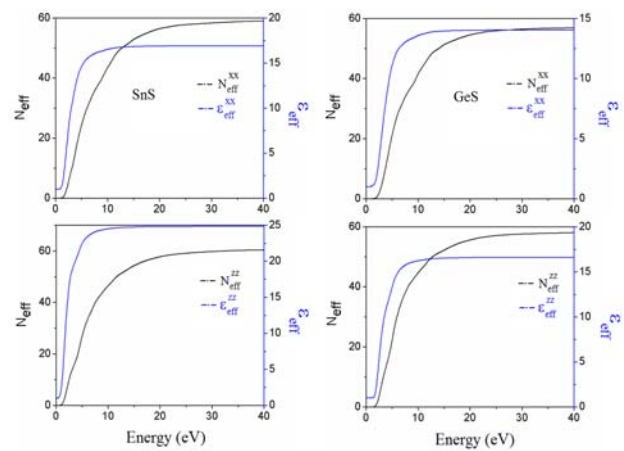


**Figure 6** Energy spectra of $N_{eff}$ and $\varepsilon_{eff}$ along the x- and z-axes.

The calculated effective number of valence electrons $N_{eff}$ and the effective dielectric constant $\varepsilon_{eff}$ are given in Fig. 6. The effective number of valence electron per unit cell, $N_{eff}$, contributing in the interband transitions, reaches saturation value at about 25 $eV$. This means that deep-lying valence orbitals participate in the interband transitions as well (see Fig. 1). The effective optical dielectric constant, $\varepsilon_{eff}$, as shown in Fig. 6, reaches a saturation value at about 10 $eV$. This means that the greatest contribu-

tion to $\varepsilon_{eff}$ arises from interband transitions between 0 and 10 $eV$.

**4 Conclusion** We studied the structural, electronic, mechanical, and optical properties of the SnS and GeS compounds using first principle DFT methods. The calculated lattice parameters are in agreement with the experimental and theoretical results. The elastic constants obtained using the "volume-conserving" technique and strain-stress relationship. Our results indicate that these compounds are mechanically stable. Due to the higher value of Young's modulus, GeS compound is relatively stiffer than SnS. In addition, the calculated bulk modulus, shear modulus, Debye temperature and wave velocity for GeS are higher than SnS. Moreover, B/G calculations for both compounds are classified as being brittle. The ionic contribution to inter atomic bonding for these compounds is dominant. We have revealed that the band structures of these compounds are a semiconductor in nature. We have examined the photon-energy dependent dielectric functions, some optical properties such as the energy-loss function, the effective number of valance electrons, and the effective optical dielectric constant along the x- and z- axes.

## References

[1] A. R. H. F. Ettema, R. A. de Groof, C. Haas, and T. S. Turner, Phys. Rev. B **46**, 7363 (1992).

[2] M. Rajagopalan G. Kalpana, and V. Priyamvadha, Bull. Mater. Sci. **29**, 25-28 (2006).

[3] A. Rathor, V. Sharma, N. L. Heda, Y. Sharma, and B. L. Ahuja, Radiat. Phys. Chem. **77**, 91-400 (2008).

[4] F. M. Gashimzade, D. A. Guseinova, Z. A. Jahangirli, and M. A. Nizametdinova, Phys. Solid State **55**, 1802-1807 (2013).

[5] U. V. Waghmare, N. A. Spaldin, H. C. Kandpal, and R. Seshadri, Phys. Rev. B **67**, 125111 (2003).

[6] H. Wiedemeier and H. G. von Schnering, Z. f. Kristallographie **148**, 295-303 (1978).

[7] B. D. Malone and E. Kaxiras, Phys. Rev. B **87**, 245312 (2013).

[8] J. M. Kohn and L. J. Sham, Phys. Rev. **140**, A1133 (1965).

[9] D. M. Ceperley and M. J. Adler, Phys. Rev. Lett. **45**, 566 (1980)

[10] P. Perdew and A. Zunger, Phys. Rev. B **23**, 5048 (1981).

[11] P. Ordejón, E. Artacho, and J. M. Soler, Phys. Rev. B **53**, R10441-R10444 (1996).

[12] J. M. Soler, E. Artacho, J. D. Gale, A. García, J. Junquera, P. Ordejón, and D. Sánchez-Portal, J. Phys.: Condens. Matter **14**, 2745-2779 (2002).

[13] O. F. Sankey and D. J. Niklewski, Phys. Rev. B **40**, 3979 (1989).

[14] N. Troullier and J. L. Martins, Phys. Rev. B **43,** 1993 (1991).

[15] F. M. Gashimzade, D. G. Guliev, D. A. Guseinova, and V. Y. Shteinshrayber, J. Phys.: Condens. Matter **4**, 1080-1091 (1992).

[16] E. Deligoz, H. Ozisik, K. Colakoglu, G. Surucu, and Y. O. Ciftci, J. Alloys Compd. **509**, 1711-1715 (2011).

[17] H. Koc, H. Ozisik, E. Deligoz, Amirullah M. Mamedov, and E. Ozbay, J. Mol. Model. **20,** 1-12 (2014).

[18] H. Koc, Amirullah M. Mamedov, E. Deligoz, and H. Ozisik, Solid State Sci. **14**, 1211-1220 (2012).

[19] D. C. Wallace, Thermodynamics of Crystals, Chap. 1 (where finite Lagrangian strains η$_{ij}$ are discussed. In the case of infinitesimal strains these reduce to our ε$_{ij}$ of classical elasticity theory) (Wiley, New York, 1972).

[20] O. Beckstein, J. E. Klepeis, G. L. W. Hart, and O. Pankratov, Phys. Rev. B **63**, 134112.1-134112.12 (2001).

[21] F. Birch, Phys. Rev. **71**, 809-824 (1947).

[22] W. Voight, Lehrbuch der Kristallphysik (Teubner, Leipzig, 1928), p. 962.

[23] A. Z. Reuss, Angew. Math. Mech. **9**, 49-58 (1929).

[24] R. Hill, Proc. Phys. Soc. London A **65**, 349-354 (1952).

[25] K.B. Panda and K.S.R. Chandran, Acta Mater. **54**, 1641-1657 (2006).

[26] P. Ravindran, L. Fast, P. A. Korzhavyi, B. Johansson, J. Wills, and O. Eriksson, J. Appl. Phys. **84**, 4891-4904 (1998).

[27] I. R. Shein and A. L. Ivanovskii, J. Phys.: Condens. Matter. **20**, 415218.1-415218.9 (2008).

[28] S. F. Pogh, Philos. Mag. **45**, 833-838 (1954).

[29] V. V. Bannikov, I. R. Shein, and A. L. Ivanovskii, Phys. Status Solidi RRL **3**, 89-91(2007).

[30] H. Fu, D. Li, F. Peng, T. Gao, and X. Cheng, Comput. Mater. Sci. **44**, 774-778 X (2008).

[31] V. Tvergaard and J. W. Hutchinson, J. Am. Chem. Soc. **71**, 157-166 (1988).

[32] D. H. Chung and W. R. Buessem, in: Anisotropy in Single Crystal Refractory Compounds, edited by F. W. Vahldiek and S. A. Mersol (Plenum Press, New York, 1968), p. 217.

[33] I. Johnston, G. Keeler, R. Rollins, and S. Spicklemire, Solids State Physics Simulations, The consortium for upperlevel physics software (Wiley, New York, 1996).

[34] O. L. Anderson, J. Phys. Chem. Solids. **24**, 909-917 (1963).

[35] E. Schreiber, O.L. Anderson, and N. Soga, Elastic constants and Their Measurements (McGraw-Hill, New York, 1973).

[36] L. Makinistian and E.A. Albanesi, Phys. Rev. B **74**, 0455206 (2006).

[37] R. Eymard and A. Otto, Phys. Rev. B **16**, 1616-1623 (1977).

[38] J. D. Wiley, A. Breitschwerdt, and E. Schönherr, Solid State Commun. **17**, 355-359 (1975).

[39] A. M. Elkorashy, J. Phys.: Condens. Matter **2**, 6195-6205 (1990).

[40] Z. H. Levine and D. C. Allan, Phys. Rev. Lett. **63**, 1719-1722 (1989).

[41] H. Koc, E. Deligöz, and A. M. Mamedov, Phys. Mag. **91**, 3093-3107 (2011).

[42] H. R. Philipp and H. Ehrenreich, Phys. Rev. **129**, 1550-1560 (1963).

[43] O.V. Kovalev, Representations of the Crystallographic Space Groups, Irreducible Representations Induced Representations and Corepresentations (Gordon and Breach, Amsterdam, 1965).

[44] L. Marton, ev. Mod. Phys. **28**, 172-183 (1956).